Nanotechnology **20** (2009) 365703 (5pp) doi:10.1088/0957-4484/20/36/365703

Identifying individual n- and p-type ZnO nanowires by the output voltage sign of piezoelectric nanogenerator

S S Lin[1,3], J H Song[1,3], Y F Lu[2] and Z L Wang[1,4]

[1] School of Materials Science and Engineering, Georgia Institute of Technology, Atlanta, GA 30332, USA
[2] State Key Laboratory of Silicon Materials, Zhejiang University, Hangzhou, 310027, People's Republic of China

E-mail: zlwang@gatech.edu

Received 19 May 2009, in final form 21 July 2009
Published 18 August 2009
Online at stacks.iop.org/Nano/20/365703

Abstract
Based on a comparative study between the piezoelectric outputs of n-type nanowires (NWs) and n-core/p-shell NWs along with the previous study (Lu *et al* 2009 *Nano. Lett.* **9** 1223), we demonstrate a one-step technique for identifying the conductivity type of individual ZnO nanowires (NWs) based on the output of a piezoelectric nanogenerator without destroying the sample. A negative piezoelectric output voltage indicates an NW is n-type and it appears after the tip scans across the center of the NW, while a positive output voltage reveals p-type conductivity and it appears before the tip scans across the central line of the NW. This atomic force microscopy based technique is reliable for statistically mapping the majority carrier type in ZnO NWs arrays. The technique may also be applied to other wurtzite semiconductors, such as GaN, CdS and ZnS.

1. Introduction

Owing to the wide band gap of 3.37 eV and the large exciton binding energy of 60 meV at room temperature, ZnO has long been recognized as an ideal material for high efficiency ultraviolet light emitting diodes (LEDs) [1]. Unintentionally doped ZnO usually exhibits n-type conduction, which is generally attributed to H or Zn interstitials or substitutional impurities such as Al_{Zn} or Ga_{Zn} [2]. Growth of p-type ZnO is of critical importance for their applications as hole injection layers in LEDs [3–5].

Recently, in addition to thin film technology, research has been carried out to grow single-crystalline p-type ZnO nanowires (NWs) [6, 7]. The p-type ZnO NWs are the fundamental building blocks for a wide range of nano-optoelectronic and nano-electronic devices, such as nano-LEDs, nanogenerators and nanopiezotronic devices [8].

For ZnO films, the n- or p-type conductivity of the sample is determined in two ways: measurements of the Hall effect and the Seebeck effect [9], which are well established techniques and convenient as it is easy to fabricate the electrodes for thin films. However, due to low dimensionality, it is hard to carry out such measurements for ZnO NWs. Up to now, the transport measurement of single NW based field effect transistors (FET) is being applied to identify the carrier type ZnO NWs [6, 7]. FET is widely applied to investigate the electronic properties of a single semiconductor NW [10]. However, considering the shallow donor nature of H [11] and the persistent photoconductivity behavior of p-type ZnO [12], the procedures used to fabricate the FET involving solution processing and photo- or electron-irradiation may change the conductivity type of the NWs. Moreover, the fabrication process is rather complex and usually destroys the NW sample. There is a great need to establish a simple method that can quickly measure the conductivity type of many NWs with good statistics and without destroying the sample for further characterization and applications.

Recently, by utilizing the piezoelectricity of semiconductive ZnO NWs, nanoscale mechanical-to-electrical energy conversion systems, known as nanogenerators, have been invented [13–16]. Realizing the presence of a piezoelectric

[3] These authors contributed equally to this work.
[4] Author to whom any correspondence should be addressed.

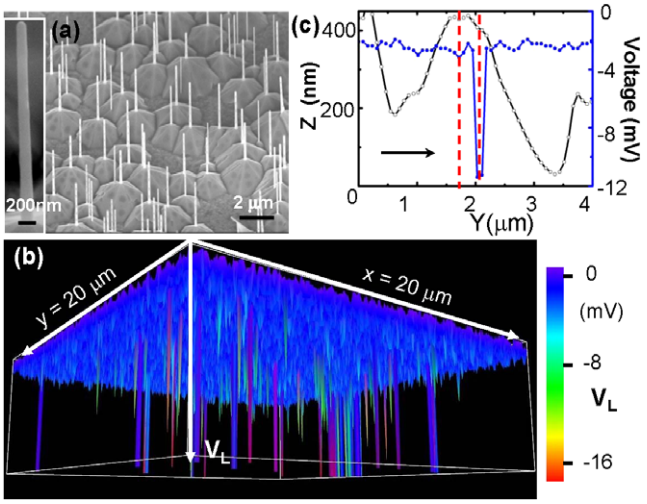

Figure 1. (a) SEM image of the as-synthesized ZnO NWs array by pulsed laser deposition; the inset shows a single NW, the diameter of which is around ∼150 nm. (b) Three-dimensional plot of output voltage of as-synthesized n-type ZnO NWs. (c) A typical line scan profile from the AFM topography (black) and the corresponding output voltage (blue). The arrowhead indicates the AFM tip scanning direction.

potential in an NW as a result of straining, a new field of nanopiezotronics [17] has been created, based on which nano-force sensors [18], piezoelectric FETs [19], and piezoelectric diodes [20] have been demonstrated. In the previous work, we have demonstrated a nanogenerator using phosphorus-doped p-type ZnO NWs array [21], which shows an opposite output electric voltage signal in contrast to that using n-type ZnO NWs. In this paper, according to more repeatable experimental results, we propose a new criterion for identifying the carrier type of individual ZnO NWs based on the piezoelectric output of an NW when it is mechanically deformed by a conductive atomic force microscopy (AFM) tip in the contact mode. The p-type/n-type shell/core NWs give positive piezoelectric outputs, while the n-type NWs produce negative piezoelectric outputs. Importantly, the results are reproducible and reliable for three sets of samples. This finding, together with the previous results on phosphorus-doped p-type ZnO NWs, firmly establishes a simple technique for quickly identifying the conductivity type of ZnO NWs without damaging the sample.

2. Experimental details

The vertically aligned n-type ZnO NWs were synthesized on silicon substrates by pulsed laser deposition (PLD). The detailed synthesis process will be systematically reported elsewhere. A nitrogen-doped p-type shell layer was deposited by plasma-free MOCVD, using diethyl zinc as the zinc source and a mixture of O_2 (13 sccm) and NO (13 sccm) as the oxygen and N doping sources. The growth temperature was fixed at 400 °C and the deposition thickness was 300–400 nm. The detailed growth procedure and characterization have been reported elsewhere [22]. Piezoelectric output measurement is based on the methodology developed by Wang and Song [13] for demonstrating the first nanogenerator. The piezoelectric responses of the NWs were measured by using an atomic force microscope (AFM) (Molecular Force Probe MFP-ED from Asylum Research) with a Pt-coated Si tip. In the AFM contact mode, a constant normal force of 80 nN was maintained between the tip and the NWs. A voltage drop across an external load of 500 MΩ connected to the AFM tip was continuously monitored while the tip scanned across the sample. In correspondence to the morphological image received, a voltage image was recorded. The Hall-effect measurements were carried out in the van der Pauw configuration (BIO-RAD HL5500PC) under a magnetic field of 0.34 T, and repeated eight times to detect the scattering data [23] for the reference film grown on a glass substrate. The morphologies of the NWs were characterized by field-emission scanning electron microscopy (FESEM: LEO 1550 FEG at 10 kV).

3. Results and discussions

Figure 1(a) shows an SEM image of the as-grown NW array by PLD and the inset displays a single NW. The as-synthesized NWs have typical diameters of ∼100–150 nm. Figure 1(b) shows the corresponding three-dimensional (3D) voltage output image after scanning an area of 20 μm × 20 μm over the n-type ZnO NW array. The n-type ZnO NWs produce negative voltage outputs when bent by a Pt-coated AFM tip. A typical profile of voltage output is shown in figure 1(c), revealing that the negative voltages are produced when the AFM tip touches the compressed side of the NWs, as indicated by the delay of the voltage peak in reference to the peak in the morphological profile [13]. This delay is a unique characteristic of an n-type ZnO NW, as explained in detail in [13]. Briefly, this delay is caused by the negative voltage output being produced only as the AFM tip touches the compressed side of the NWs.

In the second step, using the PLD grown NW arrays as a template, a thin layer (300–400 nm) of N-doped p-type ZnO was uniformly deposited on the surface of the NW array by plasma-free MOCVD [22]. The electronic properties of the p-type film grown on the glass substrate, which was grown under the exactly same conditions as the p-type shell layer was deposited on ZnO NWs, were characterized by Hall-effect measurements.

Table 1 shows the Hall-effect results of the reference N-doped ZnO film. The hole concentration is 1.12×10^{17}–7.12×10^{17} cm^{-3} as-fabricated and it is stable over two months (after two months, the hole concentration is 1.22×10^{16}–8.69×10^{16} cm^{-3} with acceptable stability). It is worth noting that the p-type layer in the core/shell should have a much higher mobility since it was grown on single-crystalline n-type NWs.

Following on, the nanogenerator based on the p-type ZnO-coated NWs will be characterized using conductive AFM. Figure 2(a) shows an SEM image of the NWs after depositing the p-type layer. The n/p core/shell NWs have typical diameters ∼400 nm, as shown in the inset of figure 2(a). The uniform and much larger diameter of the n/p core/shell NWs compared with the as-synthesized NWs demonstrate that the p-layer has been successfully grown epitaxially on

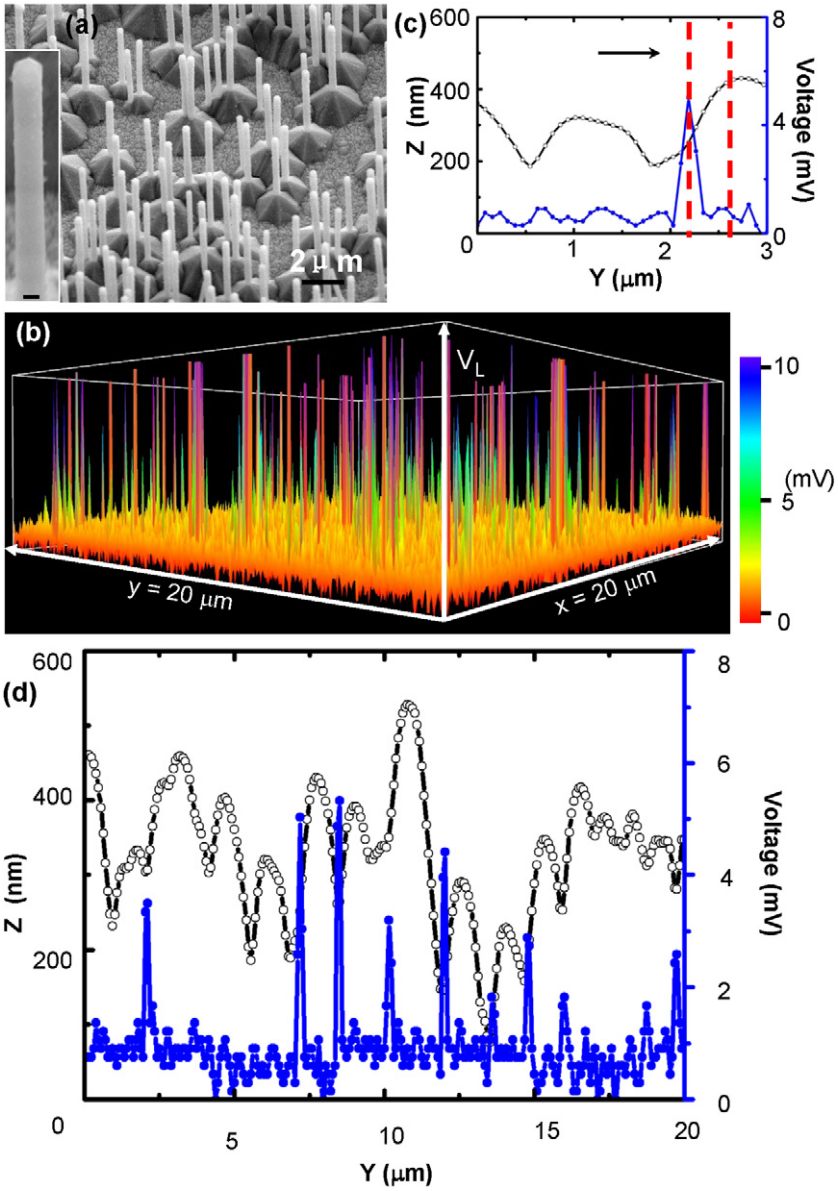

Figure 2. (a) SEM image of an n/p core/shell ZnO NW array. Inset, a single NW, the diameter of which is ∼400 nm. (b) Three-dimensional plot of output voltages of n/p core/shell ZnO NWs. (c) A typical line scan profile from the AFM topography (black) and the corresponding output voltage image (blue). The arrowhead indicates the AFM tip scanning direction. (d) A 20 μm line scan profile from the AFM topography (black) and the corresponding output voltage (blue) image; the voltage peaks were produced when the AFM tip contacted the stretched side of the NWs. The AFM tip scanning direction is from left to right.

Table 1. Hall-effect data recorded for the as-grown N-doped ZnO film sample on a glass substrate (first column). The second column is the Hall-effect data of the same sample after storage in air ambient conditions for 2 months, revealing acceptable stability.

Date	Hole concentration (cm^{-3})	Mobility ($cm^2\ V^{-1}\ s^{-1}$)	Resistivity (Ω cm)
As-fabricated	1.12×10^{17}–7.12×10^{17}	0.062–0.39	142.3
2 months later	1.22×10^{16}–8.69×10^{16}	0.078–0.56	923.1

the n-type NWs (this was also confirmed by the electron diffraction pattern, not shown here). After scanning an area of 20 μm × 20 μm over the n/p core/shell ZnO structures in the contact mode by using conductive AFM, the 3D voltage output image is produced, as shown in figure 2(b). The n/p core/shell NWs produce positive outputs throughout the entire scan range. Detailed analysis shows that the voltage peak is ahead of the peak in the morphological image in reference to the scan direction of the tip, as indicated in figure 2(c). Figure 2(d) gives further evidence that all of the positive voltage peaks are produced when the AFM tips contact the stretched side of the corresponding NWs. Compared with figure 1(b), figure 2(b) exhibits more voltage outputs in an area of 20 μm × 20 μm, which may be due to the fact

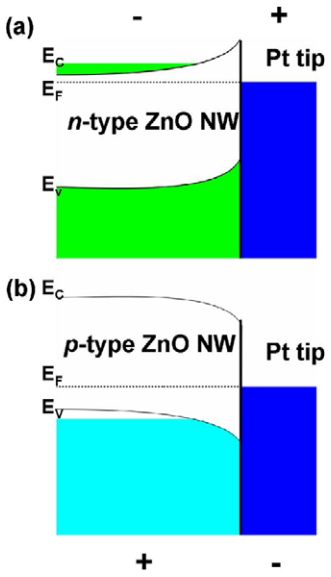

Figure 3. Energy band diagram of the contact between ZnO NWs and the Pt-coated AFM tip. (a) n-type NW and Pt tip, (b) p-type NW and Pt tip. E_C, E_V, E_F represent the conduction band, valence band and Fermi level, respectively. Forward bias is established when the Pt tip has a positive voltage (+) applied and the n-type NW has a negative voltage (−) applied, and vice versa for the p-type NW.

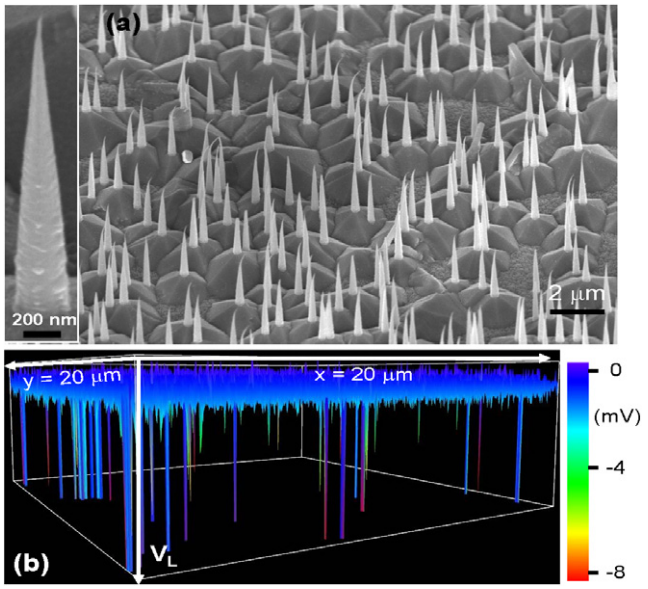

Figure 4. (a) SEM view of the ion-milled n/p core/shell ZnO NWs; inset shows a single NW, the diameter of which increases from top (∼20 nm) to the bottom (∼300 nm) monotonically.
(b) Three-dimensional plot of output voltage, showing that the negative voltage outputs recover after the p-type layers were ion milled.

that it is easier for the AFM tip to contact with the stretched sides of the NWs after p-layer deposition, due to the increased diameters. The AFM measurements were confirmed by using three sets of samples. It was found that the piezoelectric response differences between the n and n/p core/shell NWs can be reproducibly observed for an extended period of time.

The physical principle of this technique can be explained as follows. The electron affinity of ZnO is ∼4.5 eV and the work function of Pt is ∼6.1 eV. In the case of n-type ZnO NWs, the majority carriers are electrons and the Fermi level is close to the conduction band (figure 3(a)). Thus, the electrons can flow across the interface if the ZnO NWs have a lower potential. For a n-type NW being deflected by an AFM tip, the stretched side of the NW exhibits only a weak positive piezoelectric potential, as it is largely and locally screened by the electrons in the NW [24], while the compressed side of the NW preserves a negative piezoelectric potential. Therefore, a current is induced in the external load once the tip touches the compressed side of the NW, resulting in a negative voltage drop at the load in reference to the grounded end. This is why the observed output voltage peaks are negative and they are delayed in reference to the positions of the peaks in the morphological image.

In comparison, considering the band structure of the contact between p-type ZnO NWs and Pt tip when thermal equilibrium is reached, the valence band of the p-type ZnO is bent down (figure 3(b)). A positive potential should be applied at the NW side to reject the holes from the p-type ZnO NWs into the metal contact. Considering the bending geometry of the NW, this positive potential is created at the stretched side of the p-type ZnO NWs. This is why the observed output voltage is positive and the voltage peak is ahead of the peak in corresponding morphology profile.

We should point out that the positive output is only due to the p-type shell layer rather than the combined effect of the p–n junction. When the p-type/n-type shell/core NW is bent, the potential induced at the interface between the p–n junction is almost the same, hence the p–n junction should not be breakdown or forward biased. If the p–n junction were forward biased in order to observe output current, the output piezoelectric potential would be negative, which is contradictory to the experimental observation. Furthermore, three sets of samples had been examined for an extensive period of time, and highly reproducible and stable results were received, confirming the positive output is caused by the p-type shell layer.

To further demonstrate the reliability of this technique, the p-type shell layers for the n/p core/shell NWs were removed by ion milling using argon gas. The morphology of the NWs array after ion milling is shown in figure 4(a) and a single NW is displayed in the inset. Ion milling was conducted using a Gatan 600 system with the sample oriented at 15° with respect to the direction of the incident ions. Ion milling was conducted at the low-current (0.05 mA) and low-voltage (0.2–0.5 kV) condition to suppress the formation of an amorphous layer on the NW surface. The resulted NWs have a typical diameter of ∼20 nm at the tip and ∼300 nm at the bottom, reflecting that the p-type shells had been removed by ion milling, leaving the n-type ZnO NW cores. Then, AFM scanning of the processed NW arrays shows negative piezoelectric output voltages (figure 4(b)). The recovery of the negative output voltage unambiguously proves that the NWs were n-type, just as expected, demonstrating the reliability of this technique.

4. Conclusions

In summary, we have demonstrated a convenient method for identifying the majority carrier types in an individual NW. Negative voltage outputs indicate that the ZnO NWs are n-type, while positive ones reveal a p-type conductivity. This simple technique is a one-step measurement for statistically mapping the carrier type in NW arrays. In principle, this technique could also be applied to other wurtzite semiconductors, such as GaN, CdS and ZnS.

Acknowledgments

Research supported by DARPA (Army/AMCOM/REDSTONE AR, W31P4Q-08-1-0009), BES DOE (DE-FG02-07ER46394), Air Force Office (FA9550-08-1-0446), DARPA/ARO W911NF-08-1-0249, KAUST Global Research Partnership, World Premier International Research Center (WPI) Initiative on Materials Nanoarchitectonics, MEXT, Japan, NSF (DMS 0706436, CMMI 0403671). SSL gratefully acknowledges the fellowship from China Scholarship Council (CSC) (No. 2008632026). We thank Dr Jung-il Hong for his guidance in PLD synthesis.

References

[1] Tang Z K, Wong G K L, Yu P, Kawasaki M, Ohtomo A, Koinuma H and Segawa Y 1998 *Appl. Phys. Lett.* **72** 3270
[2] Meyer B K *et al* 2004 *Phys. Status Solidi* b **241** 231
[3] Tsukazaki A *et al* 2005 *Nat. Mater.* **4** 42
[4] Xu W Z, Ye Z Z, Zeng Y J, Zhu L P, Zhao B H, Jiang L, Lu J G, He H P and Zhang S B 2006 *Appl. Phys. Lett.* **88** 173506
[5] Ryu Y, Lee T, Lubguban J A, White H W, Kim B, Park Y and Youn C 2006 *Appl. Phys. Lett.* **88** 241108
[6] Xiang B, Wang P, Zhang X, Dayeh S A, Aplin D P R, Soci C, Yu D and Wang D 2007 *Nano Lett.* **7** 323
[7] Yuan G D, Zhang W J, Jie J S, Fan X, Zapien J A, Leung Y H, Luo L B and Lee C S 2008 *Nano. Lett.* **8** 2591
[8] Wang Z L 2008 *Adv. Funct. Mater.* **18** 3553
[9] Look D C 1989 *Electrical Characterization of GaAs Materials and Devices* (New York: Wiley) chapter 1
[10] Lu W, Xie P and Lieber C M 2008 *IEEE Trans. Electron Devices* **55** 2859
[11] Van de Walle C G 2000 *Phys. Rev. Lett.* **85** 1012
[12] Claflin B, Look D C, Park S J and Cantwell G 2006 *J. Cryst. Growth* **287** 16
[13] Wang Z L and Song J H 2006 *Science* **14** 312
[14] Wang X D, Song J H, Liu J and Wang Z L 2007 *Science* **316** 102
[15] Qin Y, Wang X D and Wang Z L 2008 *Nature* **451** 809
[16] Yang R, Qin Y, Dai L and Wang Z L 2009 *Nat. Nanotechnol.* **4** 34
[17] Wang Z L 2007 *Adv. Mater.* **19** 889
[18] Zhou J, Fei P, Gu Y D, Mai W J, Gao Y F, Yang R S, Bao G and Wang Z L 2008 *Nano Lett.* **8** 3035
[19] Wang X D, Zhou J, Song J H, Liu J, Xu N S and Wang Z L 2006 *Nano Lett.* **6** 2768
[20] He J H, Hsin C L, Liu J, Chen L J and Wang Z L 2007 *Adv. Mater.* **19** 781
[21] Lu M-P, Song J H, Lu M-Y, Chen M-T, Gao Y F, Chen L-J and Wang Z L 2009 *Nano Lett.* **9** 1223
[22] Zeng Y J, Ye Z Z, Lu Y F, Xu W Z, Zhu L P, Huang J Y, He H P and Zhao B H 2008 *J. Phys. D: Appl. Phys.* **41** 165104
[23] Lin S S, Lu J G, Ye Z Z, He H P, Gu X Q, Chen L X, Huang J Y and Zhao B H 2008 *Solid State Commun.* **148** 25
[24] Gao Y F and Wang Z L 2009 *Nano Lett.* **9** 1103